IEEE Access
Multidisciplinary | Rapid Review | Open Access Journal

Received March 7, 2017, accepted April 5, 2017, date of publication April 7, 2017, date of current version May 17, 2017.

Digital Object Identifier 10.1109/ACCESS.2017.2692248

A Design and Fabrication Method for a Heterogeneous Model of 3D Bio-Printing

JIANPING SHI[1,2], LIYA ZHU[2], ZONGAN LI[1,2], JIQUAN YANG[2], AND XINGSONG WANG[1]

[1]School of Mechanical Engineering, Southeast University, Nanjing 210096, China
[2]Jiangsu Key Laboratory of 3D Printing Equipment and Manufacturing, Nanjing Normal University, Nanjing 210042, China

Corresponding author: Xingsong Wang (xswang@seu.edu.cn)

This work was supported in part by the Postdoctoral Science Foundation of Jiangsu Province under Grant 1601010B, in part by the Key Technology RD Program of Jiangsu Province under Grant BE2016010, in part by the National Natural Science Foundation of China under Grant 61273243 and Grant 51407095, in part by the Natural Science Foundation of Jiangsu Province under Grant BK20150973, in part by the Scientific Research Innovation Program for Graduate of Jiangsu Province under Grant SJLX16_0282, and in part by the Science and Technology Achievement Transformation Foundation of Jiangsu Province under Grant BA2016106.

ABSTRACT Due to the advantages of control over shape and properties, multimaterial parts have potential for a broad range of biomedical engineering applications. A type of multimaterial part processing method based on digital design and manufacturing has been put forward to solve the problems associated with multimaterial part formation. A modeling platform for a heterogeneous object (HEO) part based on a material distribution control function and hierarchical contour loop was designed and utilized to characterize the material distribution in the HEO model. The hierarchical algorithm of the point color and surface texture based on the topological structure was studied and provided the basic data for the material construction area. An HEO part was fabricated using a custom-made 3-D printing system. The results showed that the digital processing method could effectively solve the problem of HEO part material definition and could realize the integrated design and manufacture of the geometry, material and function of biological parts.

INDEX TERMS 3D printing, digital jetting, heterogeneous part, multimaterial.

I. INTRODUCTION

Biological models (including human bone, tissues and organs) are usually classified as heterogeneous objects (HEOs). HEOs generally refer to functional objects that are made using a variety of materials with a definite distribution of combinations [1]–[7]. Presently, research on HEOs mainly faces two key problems: the modeling and fabrication methods for multimaterial parts [8]–[11]. The processing surface of 3D printed parts can penetrate the internal areas of parts. Additionally, there is good controllability over material accumulation on the points, lines and surfaces of the internal parts, meaning that an HEO can be quickly fabricated. With the continuing development of 3D printing technology in the biomedical field, research into multimaterial biological modeling is becoming ever more important. Using 3D printing technology, this paper studies methods for modeling multimaterial parts.

During the research process into HEO modeling methods, the current mainstream 3D model was found to only be capable of expressing the geometric information of the parts. However, in the expression of an HEO model, it is required that the model can express both geometric and material information [12]–[18]. To solve this problem, many research institutions and scholars have examined the expression of the material information in the HEO model. Jackson et al. used a finite element mesh to scan the part, with the material information expressed by the distance between the internal element node and the external boundary node [19]. Biswas et al. proposed a modeling method based on geometric fields, using the distance field to express the material distribution in multimaterial parts [20]. Siu et al. proposed a multimaterial part modeling method based on the ''gradient source.'' The method simulated the mutual diffusion between different materials in multimaterial parts. Validation was achieved using 3DP (three dimensional printing) technology to print a multicolor model [21]. A multilevel model representation method based on a spatial topological structure was suggested by Kou et al., which represented a multimaterial model using topological relations of points, lines, and surfaces, as well as body mapping [22]. Liu et al. divided the part model into an aggregate composed of a series of tetrahedral elements and proposed a concept to control its characteristics based

on local components [23]. Malinauskas et al. designed a structure with controllable microporosity; this structure was manufactured by a combination of fused filament fabrication and direct laser writing ablation, and the printed part exhibited good cellular biocompatibility [24]. Based on a layered topology storage algorithm, Choi presented a representative method of modeling functionally graded material parts [25]. Wu et al. proposed a method for defining a multimaterial part model with distance fields and realized the expression and visualization of multimaterial parts via vocal representation [26]. J Yang proposed a dynamic modeling method using point cloud data, based on the refinement of an STL (stereolithography) model and the spatial geometric modeling method for microtetrahedral reconstruction. By introducing a distribution characteristic value, a body component and a distribution vector for each material, the feature nodes in the part are affected by the material, and the geometric structure and material information for any point in the multimaterial part are realized [27].

The HEO modeling method introduced above is mainly based on the expression of the material information on the part surface and a situation in which the internal material distribution is less involved, meaning that the material information expression in the HEO is not sufficiently comprehensive.

Another HEO modeling method is introduced in this paper. First, the material information on the part surface was assigned in the Z axis. Then, the material topology was defined by 2D (two-dimensional) sections of the X-Y plane. Finally, a comprehensive material information representation method for the HEO was formed. The modeled part was eventually fabricated using a custom-made 3D printing system.

II. MULTIMATERIAL DEFINITION METHOD

The multimaterial parts mentioned in this paper refer to composite and functionally graded parts. Composite parts are a combination of multiple parts, with the material in specific components being constant. Functionally graded parts are made of continuously changing, multiphase composite parts, where the distribution of the material components follow a definite gradient function [28], [29]. The definition of the multimaterial parts included two elements: the reference characteristics and the material distribution function, which determined the distribution of each component in the parts [30]–[32].

A. REFERENCE FEATURE DEFINITION

The initial reference plane of the change of the part entity was a gradient source, which was closely linked to the definition of the material. Usually, the reference features may be chosen as points, lines, or planes such that the surface may be divided into plane and contour features. Using spherical parts as an example, the center was chosen as the reference characteristic, whereas an axis was selected as the reference characteristic for cylindrical parts. A plane may also be chosen as a reference feature, with the surface profile generally chosen as a reference feature for complex parts.

B. MATERIAL DISTRIBUTION FUNCTION DEFINITION

A material distribution function was used to represent the material properties of the forming area for multimaterial parts with the properties set to be different due to the different reference planes. We assumed that the material function was defined as $f(r_i)$. A geometric feature of a solid 3D part was selected as the reference feature, and the minimum distance r_i between the target point and the reference feature was selected as the distribution function of the independent variable of the material. To simplify the definition domain for the 3D model data, we utilized a normalization method to define the domain r_i of the material space distribution function (0, 1). The starting and ending matrix of the material were assumed to be M_1 and M_2, with the material properties of any point P within the material entity recorded as M_i. The relation between them is shown in the following formula:

$$M_i = \begin{cases} M_1 & f(r_i) \le 0 \\ f(r_i) * (M_1 - M_2) + M_1 & 0 < f(r_i) < 1 \\ M_2 & f(r_i) \ge 1 \end{cases} \quad (1)$$

In the HEO 3D printing system, the material distribution function $f(r_i)$ may be mapped to the point coordinates of a geometric space using the known geometric coordinates of the HEO model and by combining them with the material distribution function. The material distribution function may be a linear or nonlinear function and can be expressed as follows:

$$f(r_i) = \lambda \quad (2)$$

$$f(r_i) = \alpha * r_i + \lambda \quad (3)$$

$$f(r_i) = \alpha * r_i^2 + \beta r_i + \lambda \quad (4)$$

$$f(r_i) = \alpha * \sin(\beta r_i) + \lambda \quad (5)$$

where α, β and λ are constant coefficients, r_i is the ratio of the current distance to the reference total distance, $f(r_i)$ is the material distribution function, and equations (2), (3), (4) and (5) represent constant, linear, nonlinear and periodic functions respectively.

C. PROFILE FAMILY DEFINITION

The 3D model was layered based on the topological structure. A series of 2D ring slice data sets were derived from slicing the 3D model into a .PLY (polygon file format) format, with the data of each slice being represented by a series of contours, and the contour of each layer being composed of a plurality of the outer contour ring and a plurality of the inner contour loop. The 3D model O_L composed of each contour ring layer may be expressed as shown in formula (3):

$$O_L = \{(L_i), i = 1, 2 \cdots l\} \quad (6)$$

where l represents the total number of layered slices in the current model, and L_i represents the collection of the current hierarchical outline ring; L_i may be expressed by formula (4):

$$L_i = \left\{\left(C_{i,j}\right), j = 1, 2 \cdots c\right\} \quad (7)$$

where $C_{i,j}$ represents the contour ring of section j of the first i in the current model, and c represents the total number of current layered contour rings.

D. OFFSET SUB REGION DEFINITION

To express the material change between the contour rings in the X-Y plane, 2D contour groups are divided into several contour sub areas, with the corresponding contour loop material composition set for each sub region. Based on the outline ring, the entity region between each outline ring may be conveniently determined. In this paper, the solid domain of the 2D model was divided into several sub regions. The resolution of the profile discrete offset was determined by the shortest distance between the two contours and the resolution of the 3D printer, as shown in formula (5):

$$N_R = int(\frac{L_S}{D_N}) \tag{8}$$

where N_R represents the number of discrete entities in the sub region, L_S represents the shortest distance between the two contour rings constituting the entity region, and D_N represents the diameter of the nozzle.

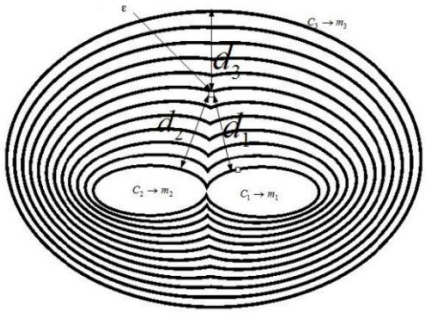

FIGURE 1. Relationship between the material distribution and the locations of the points.

E. CONTOUR OFFSET POINT MATERIAL DEFINITION

The offset algorithm for the 2D profile solid region depends on the shape of the current contour. If the contour shape is a standard shape, the equidistant points of the external contour can be offset from the inner contour to form an internal area. However, if it is an irregular shape, the offset point position is decided using the corresponding outer and inner contour positions together, and the number of offset points is determined by the number of intersecting contour rings, as shown in Fig. 1.

For calculating each unit-specific material component, the center of the unit can be used as a reference position, and the material group depends on the distance between each contour. Assuming that the 3D model is composed of β material types, the material group value $M(\varepsilon)$ for a point is decided by the point and material associated with the contour ring at the point, with the specific calculation shown in formula (6):

$$M(\varepsilon) = \sum_{i=1}^{\beta} m_i(C_i) w_i(\varepsilon) \tag{9}$$

where β represents the total number of contour rings, $m_i(C_i)$ represents the color attribute value of the i^{th} raw material in the C_i contour ring, and $w_i(\varepsilon)$ represents the weighted value of the i^{th} material of the current point ε, as shown in formula (7):

$$w_i(\varepsilon) = \frac{\prod_{k=1,k\neq i}^{\beta} d_k(\varepsilon)}{\sum_{j=1}^{\beta} \prod_{k=1,k\neq i}^{\beta} d_k(\varepsilon)} \tag{10}$$

where $d_k(\varepsilon)$ represents the shortest distance between the current point ε to the first k contour ring, k is in the range of $(1, 2, 3 \cdots \beta)$, and $w_i(\varepsilon)$ meets the condition that the weighting for all the material sums to 1.

III. HEO MODELING METHOD

A. MODELING ALGORITHM OF THE MODEL SURFACE MATERIAL DISTRIBUTION IN THE Z AXIS

The main idea behind the modeling method for the model surface material distribution in the Z axis is that the geometric characteristics of the parts are selected as material distribution reference features, and the distribution function of the material component is established along the normal direction of the reference features such that the value of the material component is imparted to the triangular surface of the model. The method for 3D model representation of multimaterial parts is based on the .PLY data format in this paper.

1) PROCESS DESCRIPTION OF THE HEO MODELING ALGORITHM FOR THE Z AXIS

Step 1: Read the .PLY data file for the HEO. The minimum bounding box is then established for the HEO model as $(x_{min}, x_{max}, y_{min}, y_{max}, z_{min}, z_{max})$.

Step 2: Initialize the .PLY data file and establish null data sets, so the value of the vertex RGB (red, green, blue) color attribute for the model facet triangle is initialized to (0, 0, 0).

Step 3: Set the material distribution reference feature. According to the geometric features of the triangle vertex reference area, the color attribute value generated corresponds to the vertex material data.

Step 4: Set the material space distribution function for the HEO model. The appropriate material space distribution function is mapped to the spatial node of the HEO model along the normal reference direction.

Step 5: Read the .PLY data file geometric data information and the color space information, and output the .PLY file.

2) VERIFICATION OF MODELING ALGORITHM

A design and modeling example using a vase and based on a material distribution function is presented to verify the reliability and effectiveness of the HEO modeling method. The vase parameters are shown in Table 1.

The specific implementation process is as follows: the forward modeling method is used to geometrically model the vase entity and establish the geometrical and topological structure of the vase model. The .PLY file format preserves the triangular mesh nodes of both the inside and outside surfaces of the vase. Then, the spatial position and topological

TABLE 1. Vase parameters.

Model	Points	Lines	Triangle	Reference Feature	Material Distribution Function
vase	3115	9339	6226	X-Y plane	linear function nonlinear function periodic function

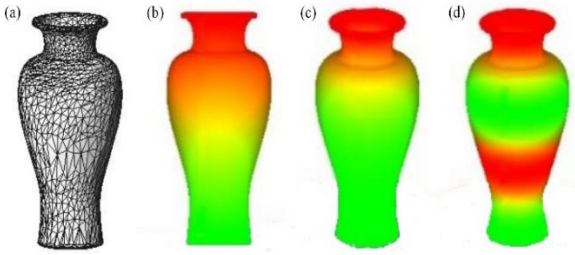

FIGURE 2. Function distribution of the HEO model in the Z axis: (a) surface triangular mesh vase model; (b) material distribution using a linear function; (c) material distribution using a nonlinear function; and (d) material distribution using a periodic function.

structure of the vase are established. The vase .PLY files are then read and initialized. The RGB values of the vase material information are set to zero. The bottom surface of the vase is set as a reference plane. The material distribution function is created along the normal direction of X-Y features. In addition, the independent variable is the spatial distance from a point to the reference. Finally, the material distribution function of the vase is set as constant, linear, nonlinear and periodic functions. The results are presented in Fig. 2.

B. MODELING ALGORITHM OF MODEL SURFACE MATERIAL DISTRIBUTION IN THE X-Y PLANE

The X-Y hierarchical profile in this paper is generated from a 2D intersection contour ring, which is output from the multilayer data processing of the HEO model. The contour ring is divided into contour families according to the definition of the contour ring family. The specific steps for this activity are as follows:

1) PROCESS DESCRIPTION FOR THE HEO MODELING ALGORITHM FOR THE X-Y PLANE

Step 1: Initialize the outline loop list: CLIST.

Step 2: Set the order number for the current hierarchical outline family: $i = 1$.

Step 3: Set the number for the current slice bias sub region: $i = 1$.

Step 4: Select the current offset type from the outer outline ring to the internal contour ring based on the requirements of the customer.

Step 5: Insert the bias contour loop into the outline ring list.

Step 6: Determine whether the number (j) of sub regions in the current slice offset is less than or equal to the total number (N_R) of offsets in the 2D region with an outline family as the boundary. If the condition is less than equal, Step 4 is executed; otherwise, perform the next step.

Step 7: Determine whether the number (i) of the outline families of the current layer is less than or equal to the number (p) of the total outline family of the current layer.

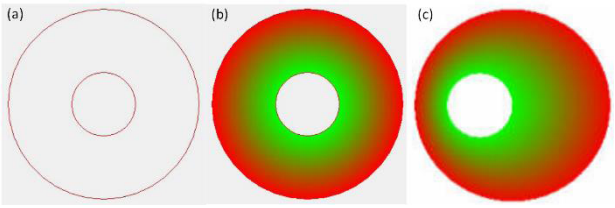

FIGURE 3. Material distribution for the HEO model in the X-Y plane: (a) the sliced contour of the 360th layer of the model; (b) material distribution in the 360th layer; and (c) material distribution of contour for a uniquely shaped region.

2) VERIFICATION OF MODELING ALGORITHM

In this paper, the contour interface for a hierarchical region of a vase is taken as an example. Based on the material distribution function, a design and modeling example using the multimaterial vase layered section is illustrated.

The material distribution modeling of the X-Y plane layered profile was based on processing the data of the multimaterial parts. Using 3D printing, the 2D material topology operation was calculated from a sliced contour of the model. According to layered profile data in the Z axis, the geometric coordinates and the color attribute values of the 360 intersecting points in the model were read, and the results are shown in Fig. 3. The color attribute value of the external contour was set as the starting point, and the material distribution function of the external contour of the target contour was set for the linear function. The color value of the target contour was (0, 255, 0). The outer contour was offset 200 times to the inner contour, and the contour offset results are shown in Fig. 3.b.

IV. LAYERED PROCESSING FOR HEO PARTS

A topological layering algorithm based on the .PLY file format is proposed in this work. The main idea of the algorithm is as follows. The entire triangle is divided into groups according to how the film intersects the triangle, which is based on topological relations. There are three principal tasks. First, a singular point is addressed using a microtriangle vertex with the delamination direction determined using two factors: the number of fretting vertices and the support volume. Second, the HEO model is rapidly layered by means of global grouping and local topological layering. Third, internal and external contour areas are automatically recognized by optimizing the local topology algorithm.

A. GLOBAL INTERSECTION FILTER FOR THE TRIANGULAR PATCHES

The first step in the slicing algorithm is sorting the triangles intersecting the slicing surface. Fig. 4 shows example models of local triangle sections and slice intersections. The entire

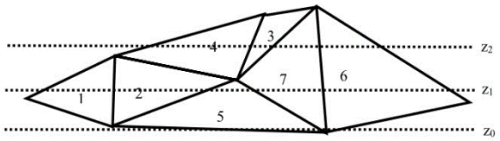

FIGURE 4. Intersections of slicing planes and local triangles of the model.

TABLE 2. Intersection results of the slicing planes and triangles.

Slicing Plane Height	Triangle Numbers
$Z=Z_0$	5, 6, 7
$Z=Z_1$	1, 2, 5, 6, 7
$Z=Z_2$	3, 4, 6, 7

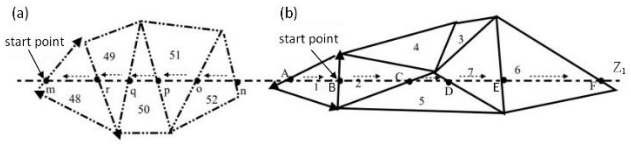

FIGURE 5. Intersections of the slicing plane and triangles of the inner and outer surfaces of the model: (a) inner intersections and (b) outer intersections.

intersection triangle grouping algorithm is introduced in the example in Fig. 4, which shows the intersections of the slicing planes and local triangles of the model. The hypothetical model consists of seven local triangles that are stored unfixed. Each triangle may be indexed with three triangle vertex coordinates. A judgment on whether the slicing plane intersects the triangles is implemented according to the three triangle vertex coordinates in the Z axis located on a side piece. In Fig. 4, the three vertices of triangle 4 are on the same side as the layer height Z_1. As a result, the slicing plane with a height $Z=Z_1$ does not intersect triangle 4. However, the slicing plane intersected triangles 1, 2, 5, 6 and 7. The intersection results of the slicing planes and triangles are listed in Table 2.

B. LOCAL TOPOLOGY SLICING

The triangles and three vertices of the .PLY file data are stored using no specific rules. This is a key factor for the slicing speed to quickly reconstruct the intersections of the triangle sections and the slicing planes. As shown in Fig. 6, we assume that the dotted line represents the inner triangles of the model, and the normal vector of the initial 48 triangles points to the internal model according to the right-hand rule. The solid line represents the outer triangles. The stored list sequence for the triangle slice intersections is (1, 2, 5, 7, 6, 48, 49, 50, 51 and 52).

In the local topology reconstruction algorithm, the initial edge selection relation may influence the proper construction of the hierarchical contour. The initial intersection edge is selected according to the initial intersection selection rule. The initial triangle vertices in the inner and outer contours are stored using the right-hand rule. The vector edge whose

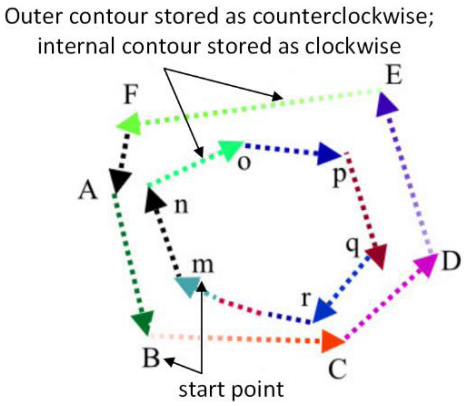

FIGURE 6. Sketch of a colored contour section.

starting point is located under the slicing plane and whose ending point is located upon the slicing plane is selected as the initial edge. Fig. 5 shows that m is the internal contour intersection and that B is the external contour intersection. Based on the local topological layered algorithm, the internal contour storage intersection number order is m-n-o-p-q-r, and the external contour storage order is B-C-D-E-F-A.

According to the proposed method based on global grouping and the intersections of the local topological stratification, the intersection points are colored, and the output contours are arranged in a specific order, as shown in Fig. 6.

V. HEO MODEL FABRICATION BASED ON A DIGITAL JETTING PROCESS

Digital micro-jetting technology is a process in which a portion of liquid material breaks away from the parent material in a short time as the result of an excitation. Then, a discrete droplet or a continuous jet stream is formed and sprayed from a nozzle at a specified position with a certain response rate and speed. Finally, the formation of a solid 3D part is realized. A schematic of the printing process is shown in Fig. 7.

Prior to printing, forward and reverse modeling methods are used to obtain a 3D model of an object, such as a liver, as shown in Fig. 8.a. The corresponding material information is provided to the geometric model, which is saved in the .PLY file format with color information indicating the location of lesions, as shown in Fig. 8.b. Fig. 8.c shows the printed diseased liver part.

Via the slicing algorithm described in this paper, a 3D color .PLY model may be sliced using a thickness of 0.1 mm. The output resolution was set to 600x600 dpi. The 2D profile of the output file was saved using a .tiff format file. Here, the output file of the 83rd slicing layer of the HEO model is taken as an example. The output data may be identified using a 3DP system via an RIP (raster image processor). Afterwards, the RIP files can be imported into the 3DP software. The results from the sliced contour with and without any internal material distributions are shown in Figs. 9.a.b.

Initially, the printing software automatically sends the data signal to the control board of the printing system. According to the data provided from the 2D contour section,

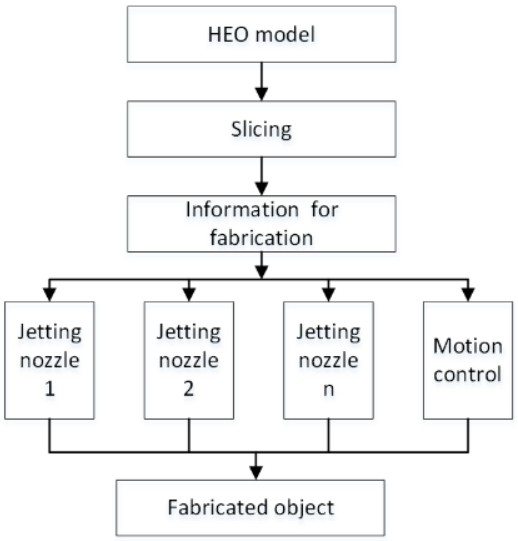

FIGURE 7. Schematic of the printing process.

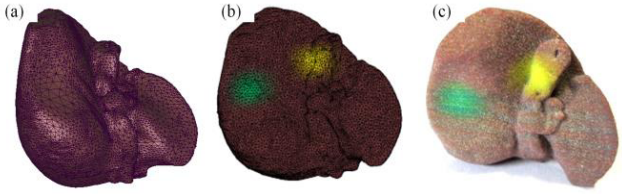

FIGURE 8. Modeling and fabrication of an HEO: (a) geometric model of the HEO; (b) HEO model with material information; and (c) printed HEO part.

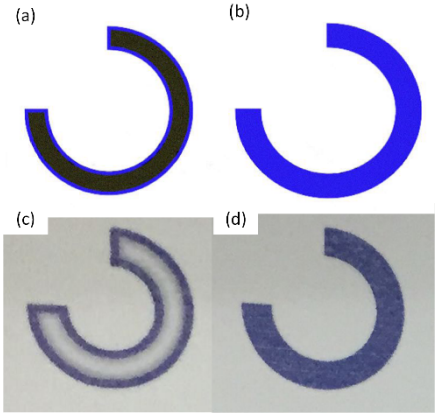

FIGURE 9. Images of the sliced and printed contour of the 83rd sliced layer: (a) sliced contour without any internal material distribution; (b) sliced contour with an internal material distribution; (c) printed contour without any internal material distribution; and (d) printed contour with an internal material distribution.

the nozzle is commanded to move to the corresponding position to spray the corresponding material. The forming effects are illustrated in Figs. 9.b.c, and the final fabricated HEO part is shown in Fig. 8.c.

VI. CONCLUSION

In this paper, a modeling platform for an HEO part based on a material distribution control function and a hierarchical contour loop was designed. The platform consists of two components in the Z axis direction. The material distribution at the model surface grid node is determined by the material control function. In the X-Y direction, and based on the concept of material laminated manufacturing via 3DP, the material control function is mapped using a 2D slice contour, and material-specific sub areas are formed to create a representation of the material distribution in the internal portion of the HEO.

Additionally, according to the model, a hierarchical algorithm for the point color and surface texture based on a topological structure was studied. The algorithm not only determines the surface profile value but also effectively identifies and reconstructs the internal and external contours of a layered 2D section, which provides the basic data for the material construction area and enables ideal slicing. Using homemade heterogeneous material printing equipment, an HEO model was designed and fabricated. The results show that the model has a superior ability to characterize multi-material parts. The modeling and printing methods used here have promise for applications in the preparation of multimaterial bio-models.

REFERENCES

[1] A. Pasko, V. Adzhiev, and P. Comninos, *Heterogeneous Objects Modelling and Applications: Collection of Papers on Foundations and Practice*. Berlin, Germany: Springer-Verlag, 2008.
[2] N. Li, J. Yang, C. Feng, J. Yang, L. Zhu, and A. Guo, "Digital micro-droplet ejection technology-based heterogeneous objects prototyping," *Int. J. Biomed. Imag.*, vol. 4, no. 1, pp. 1–7, 2016.
[3] Y.-D. Zhang *et al.*, "Fractal dimension estimation for developing pathological brain detection system based on Minkowski-Bouligand method," *IEEE Access*, vol. 4, pp. 5937–5947, 2016.
[4] S.-H. Wang *et al.*, "Multiple sclerosis detection based on biorthogonal wavelet transform, RBF kernel principal component analysis, and logistic regression," *IEEE Access*, vol. 4, pp. 7567–7576, 2016.
[5] L. Na, Y. Jiquan, C. Jihong, and Q. Weixing, "Digital printing of the thin film sensor with sharp edge based on electrodynamics 3DP," *Open Elect. Electron. Eng. J.*, vol. 8, no. 1, pp. 573–579, 2014.
[6] Y. S. Zhang *et al.*, "3D bioprinting for tissue and organ fabrication," *Ann. Biomed. Eng.*, vol. 45, no. 1, pp. 148–163, 2017.
[7] W. J. Jin, J.-S. Lee, and D.-W. Cho, "Computer-aided multiple-head 3D printing system for printing of heterogeneous organ/tissue constructs," *Sci. Rep.*, vol. 6, no. 247, 2016, Art. no. 21685.
[8] D. Shi, K. Liu, X. Zhang, H. Liao, and X. Chen, "Applications of three-dimensional printing technology in the cardiovascular field," *Int. Emerg. Med.*, vol. 10, no. 7, pp. 769–780, 2015.
[9] J. Zheng, "A multi-material 3D printing system and model-based layer-to-layer control algorithm for ink-jet printing process," Ph.D. dissertation, Rensselaer Polytech. Inst., Gradworks, Regina, SK, Canada, 2014.
[10] Y.-D. Zhang *et al.*, "Facial emotion recognition based on biorthogonal wavelet entropy, fuzzy support vector machine, and stratified cross validation," *IEEE Access*, vol. 4, pp. 8375–8385, 2016.
[11] S. Ready, G. Whiting, and T. N. Ng, "Multi-material 3D printing," in *Proc. NIP Digit. Fabrication Conf.*, 2014, pp. 120–123.
[12] J. Shi *et al.*, "The modeling and digital micro-droplet injection technology of heterogeneous material part," *J. Nanjing Normal Univ.*, vol. 12, no. 1, pp. 10–14, 2012.
[13] P. Sitthi-Amorn *et al.*, "MultiFab: A machine vision assisted platform for multi-material 3D printing," *ACM Trans. Graph.*, vol. 34, no. 4, p. 129, 2015.
[14] R. B. Wicker, F. Medina, and C. Elkins, "Multiple material micro-fabrication: Extending stereolithography to tissue engineering and other novel applications," in *Proc. 15th Annu. Solid Freeform Fabrication Symp.*, Austin, TX, USA, 2004, pp. 754–764.
[15] R. Holtrup "XZEED DLP. A multi-material 3D printer using DLP technology," Univ. Twente, Enschede, The Netherlands, Tech. Rep., 2015.

[16] Q. Ge, A. H. Sakhaei, H. Lee, C. K. Dunn, N. X. Fang, and M. L. Dunn, "Multimaterial 4D printing with tailorable shape memory polymers," *Sci. Rep.*, vol. 6, pp. 1–11, Aug. 2016.
[17] K. Dimitri, S. Manuel, and A. R. Studart, "Multimaterial magnetically assisted 3D printing of composite materials," *Nature Commun.*, vol. 6, Jul. 2015, Art. no. 8643.
[18] P. Regenfuss *et al.*, "Principles of laser micro sintering," *Rapid Prototyping J.*, vol. 13, no. 4, pp. 204–212, 2013.
[19] T. R. Jackson, H. Liu, N. M. Patrikalakis, E. M. Sachs, and M. J. Cima, "Modeling and designing functionally graded material components for fabrication with local composition control," *Mater. Design*, vol. 20, nos. 2–3, pp. 63–75, 1999.
[20] A. Biswas, V. Shapiro, and I. Tsukanov "Heterogeneous material modeling with distance fields," *Comput. Aided Geometric Design*, vol. 21, no. 3, pp. 215–242, 2004.
[21] Y. K. Siu and S. T. Tan, "'Source-based' heterogeneous solid modeling," *Comput.-Aided Design*, vol. 34, no. 1, pp. 41–55, 2002.
[22] X. Y. Kou and S. T. A. Tan, "Heterogeneous object modeling: Review," *Comput.-Aided Design*, vol. 39, no. 4, pp. 284–301, 2007.
[23] H. Liu *et al.*, "Methods for feature-based design of heterogeneous solids," *Comput.-Aided Design*, vol. 36, no. 12, pp. 1141–1159, 2004.
[24] M. Malinauskas, "3D microporous scaffolds manufactured via combination of fused filament fabrication and direct laser writing ablation," *Micromachines*, vol. 5, no. 4, pp. 839–858, 2014.
[25] S. H. Choi and H. H. Cheung, "A topological hierarchy-based approach to layered manufacturing of functionally graded multi-material objects," *Comput. Ind.*, vol. 60, no. 5, pp. 349–363, 2009.
[26] X. Wu, W. Liu, and M. Y. Wang, "A CAD modeling system for heterogeneous object," *Adv. Eng. Softw.*, vol. 39, no. 5, pp. 444–453, 2008.
[27] J. Yang *et al.*, "Point cloud based on dynamic representation for heterogeneous objects," *Chin. J. Mech. Eng.*, vol. 23, no. 20, pp. 2453–2458, 2012.
[28] Z. Li *et al.*, "Processing and 3D printing of gradient heterogeneous biomodel based on computer tomography images," *IEEE Access*, vol. 4, pp. 8814–8822, 2016.
[29] L. Hou, W. Zhang, and L. Zhu, "Preparation of paper micro-fluidic devices used in bio-assay based on drop-on-demand wax droplet generation," *Anal. Methods*, vol. 6, no. 3, pp. 878–885, 2014.
[30] X. Qian, "Adaptive slicing of moving least squares surfaces: Toward direct manufacturing of point set surfaces," *J. Comput. Inf. Sci. Eng.*, vol. 8, no. 3, pp. 433–442, 2008.
[31] D. Chakraborty and A. R. Choudhury, "A semi-analytic approach for direct slicing of free form surfaces for layered manufacturing," *Rapid Prototyping J.*, vol. 13, no. 4, pp. 256–264, 2007.
[32] H. J. Kim, K.-H. Wie, S.-H. Ahn, H.-S. Choo, and C.-S. Jun, "Slicing algorithm for polyhedral models based on vertex shifting," *Int. J. Precision Eng. Manuf.*, vol. 11, no. 5, pp. 803–807, 2010.

JIANPING SHI received the B.S. degree in mechanical engineering in 2010, and the M.S. degree in electronic engineering from Nanjing Normal University, China, in 2013. He is currently pursuing the Ph.D. degree with Southeast University. He is currently a Researcher with the Jiangsu Key Laboratory of 3D Printing Equipment and Manufacturing. His current research interests include 3-D printing methods and 3-D bio-printing for tissue engineering.

LIYA ZHU received the B.S. degree from the Wuhan University of Technology, and the Ph.D. degree from the Nanjing University of Aeronautics and Astronautics, China. She is currently a Lecturer with Nanjing Normal University and the Jiangsu Key Laboratory of 3D Printing Equipment and Manufacturing. Her current research interests include 3-D bio-printing for tissue engineering.

ZONGAN LI received the B.S. degree in mechanical engineering from the Nanjing University of Science and Technology, China, in 2009, and the Ph.D. degree in instrument science and technology from the Nanjing University of Science and Technology, China, in 2015. He is currently a Post-Doctoral Researcher with Southeast University and the Jiangsu Key Laboratory of 3D Printing Equipment and Manufacturing. His current research interests include developing 3-D model reconstruction software based on computed tomography images and 3-D bio-printing for tissue engineering.

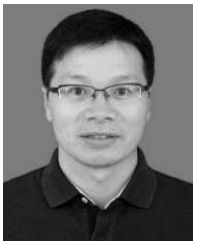

JIQUAN YANG received the B.S. degree in mechanical engineering and the Ph.D. degree in instrument science and technology from the Nanjing University of Science and Technology, China. He is currently a Professor with Nanjing Normal University and the Jiangsu Key Laboratory of 3D Printing Equipment and Manufacturing. His current research interests include 3-D printing.

XINGSONG WANG received the B.S. and M.S. degrees from Zhejiang University, Hangzhou, China, in 1991, and the Ph.D. degree from Southeast University, Nanjing, China, in 2000. He is currently a Full Professor with the School of Mechanical Engineering and the Department Head of the Department of Mechatronics with Southeast University. His current research interests include control theory with applications in precision computer numerical control machine tools, advanced mechatronics with applications in biomedical engineering, and tendon-sheath transmission theory with applications in rescue robots.